

CTuJ1 Fig. 3. (a) Histograms showing how the mean and standard deviation of the Raman PDG decrease as the PMD is increased from 0.03 to 0.09 to 0.15 ps/km^{1/2}; (b) and (c) show the mean PDG and the standard deviation of the Raman gain versus PMD (and 1/PMD) for a 10-km Raman amplifier (where the PDG and gain are normalized to the average gain).

nal power fluctuations are monitored with an optical spectrum analyzer (OSA).

Within the amplifier, 11 polarization controllers (PCs) are placed at approximately 800 m intervals. By changing these PCs between measurements, we induced random variations in the polarization mode coupling within the transmission fiber that would otherwise only occur over a long period of time. We verified this technique by taking 500 samples of instantaneous differential group delay (DGD) at our signal wavelength while randomly changing the PCs between measurements. The resulting DGD distribution (fig. 1) closely approximates the expected Maxwellian and yields an average PMD of 0.06 ps/km^{1/2}. It should also be noted that the PDL of our setup is ≤ 0.33 dB, which is about 1 dB less than our average PDG.

Results

Fig. 2(a) shows the measured PDG distribution. The 11 PCs were varied randomly between each of the 500 samples. During each measurement, the output signal power was monitored while the input signal SOP was varied randomly. The maximum achieved power fluctuation determines the PDG since the average Raman gain, which was also measured at each data point, remained constant at 3.4 ± 0.15 dB (variation due to PDL). To further verify our measurement technique, another 500 samples were taken without changing the 11 PCs at all (over a period of only four hours to avoid the natural evolution of polarization coupling within the fiber). The resulting PDG remained constant within ± 0.2 dB, adding validity to our method. Fig. 2(b) shows the cumulative distribution functions (cdf) for the

measured and simulated PDG for 0.06 ps/km^{1/2} PMD. Note the simulated and experimental results closely agree. Similarly, figs. 2(c) and (d) show the measured and simulated distributions of the instantaneous Raman gain. Again, the simulated and experimental results are in agreement.

Since our experimental results are presently limited to only a single PMD value (we are looking for higher PMD fibers to further our experiments), the simulation was used to investigate how the PDG statistics vary for different values of PMD. Our simulation models a fiber with PMD as a series of 1000 equal length sections with random polarization mode coupling between them. The Raman gain of each section depends on the relative polarizations of the signal and pump. Fig. 3(a) shows that even modest increases in the PMD reduce both the average and spread of the PDG distribution. Fig. 3(b) shows the normalized variation of the mean PDG versus PMD. The results show that a total PMD of 0.66 ps ($0.2 \text{ ps/km}^{1/2} \times (10 \text{ km})^{1/2}$) is enough to reduce the mean PDG to as low as 10% of the average gain. Fig. 3(c) shows the normalized variation of the standard deviation of the Raman gain versus PMD. Also note that the constant slope in fig. 3(b) shows that the product of the mean PDG and the PMD of the link remains constant, as does $\sigma_{\text{Gain}} \times \text{PMD}$ (fig. 3(c)).

References

1. R.H. Stolen, "Polarization effects in fiber Raman and Brillouin lasers," IEEE J. Quantum Electronics, QE-15, 1157 (1979).
2. D. Mahgerefteh, H.Y. Yu, D.L. Butler, J. Goldhar, D. Wang, E. Golovchenko, A.N. Piliptskii, C.R. Menyuk and L.J. Joneckis, "Effect of

randomly varying birefringence on the Raman gain in optical fibers," CLEO '97, CThW5 (1997).

3. J. Zhang, V. Dominic, M. Misyk, S. Sanders, and D. Mehuys, "Dependence of Raman Polarization Dependent Gain on Pump Degree of Polarization at High Gain Levels," OAA '00, OMB4 (2000).
4. H. Suzuki, N. Takachio, H. Masuda and M. Koga, "50 GHz spaced, 32×10 Gbit/s dense WDM transmission in zero-dispersion region over 640 km of dispersion-shifted fibre with multiwavelength distributed Raman amplification," Electronics Letters, Vol. 35, No. 14, pp. 1175-1176 (1999).

CTuJ2

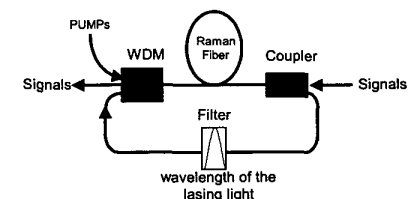
10:30 am

Dynamic gain control for discrete Raman fiber amplifier

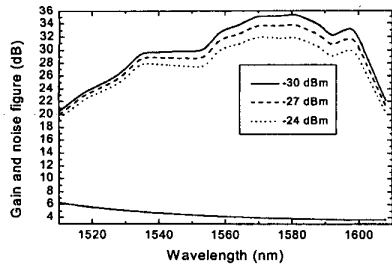
Xiang Zhou, Chao Lu, Ping Shum, Hossam H.M. Shalaby and Teehiang Cheng, Optical network group, Nanyang Technological Univ., School of Electrical and Electronic Engineering, Block S2, NTRC, Nanyang Avenue, Singapore 639798; Email: ezhou@ntu.edu.sg

Among the various competing candidates for next generation fiber amplifier, Fiber Raman amplifiers (RFAs) are recently attracting many researchers' attention in DWDM system due to their distinctive flexibility in bandwidth designs and growing maturity of high power pump module technologies.¹⁻³ Despite the simplicity of the architecture of a Raman amplifier, many issues, such as gain flattening, double Rayleigh scattering noise, ASE noise must be considered in the design of the amplifier and the systems that use them. Further more, in the design of optical amplified link for DWDM application in a network scenario, the number and the power level of the input channels may vary randomly in time, therefore it is also essential to stabilize the amplifier gain profile. In this paper, We investigated the issue of dynamic gain control for Raman fiber amplifier through theoretical simulation. The basic idea is similar to a gain-clamped EDFA. That is, by introducing an all-optical feedback lasing signal sustained by the amplifier itself, we hope that the gain profile of a RFA can be clamped to the desired level. To our knowledge, this is the first time this issue is being dealt with.

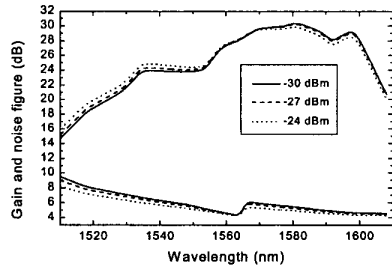
The proposed gain_clamp Raman amplifier is shown in Fig. 1, where both the pumps and the lasing light are designed to counterpropagate against the signals. Such a design is necessary to compress the channel crosstalk in DWDM systems since the intensity of the lasing light can be very strong in some time. The stable performance of the proposed gain-clamped RFA was



CTuJ2 Fig. 1. Diagram of Raman fiber amplifier with automatic gain control



CTuJ2 Fig. 2. Gain and noise figure of a conventional Raman fiber amplifier.



CTuJ2 Fig. 3. Gain and noise figure of a gain-clamped Raman fiber amplifier.

simulated. In our simulation, we considered the pump-pump, pump-signal, signal-signal, pump-lasing light, and signal-lasing light interactions, temperature dependent ASE noise and Rayleigh backward scattering noise. The parameters used in our simulation are given as follows. Pump wavelength: 1425 nm, 1455 nm and 1480 nm. The corresponding pump power is 1.6 w, 0.3 w, and 0.4 w, respectively. 100 incoming signal (1510 nm to 1610 nm, 1 nm separation). Fiber length = 6 km and the fiber effective area = 50 μm^2 . The Raman gain profile of silicon fiber was chosen from.⁴

Fig. 2 gives the calculated gain spectrum profile and noise figure of a RFA without gain control. We can see that, when the incoming signal power (each channel) varying from -24 dBm to -30 dBm, the signal gain fluctuation can be more than 3.5 dB. However, when we introduce a lasing light as is shown in Fig. 1, the gain fluctuation can be compressed. Such a result is clearly shown in Fig. 3, where the lasing wavelength was chosen to be 1565 nm. It can be seen that, gain variation compression of more than 3 dB can be obtained over 45 nm bandwidth (from 1545 to 1590). However, when the lasing wavelength is chosen to be shorter or longer, our simulation shows that, the gain-clamping effects becomes worse. For example, for lasing wavelength at 1540 nm or 1590 nm, the calculated 3 dB gain compression bandwidth is less than 20 nm. In addition, our calculation shows that, the optimal lasing wavelength is dependent on the Raman gain profile, fiber length and pump powers.

Similar to the case of a gain-clamped EDFA, the noise figure will increase when a lasing light is introduced.

References

1. OSA IEEE: F. Koch, S.A.E. Lewis, S.V. Chernikov, J.R. Taylor, "Broadband gain flat-

tened Raman amplifier to extend operation in the third telecommunication window", OFC (Baltimore, USA, 2000), paper FF3-1.
 2. OSA, IEEE: Hiroji Masuda, "Review of wide-band hybrid amplifier", OFC (Baltimore, USA, 2000), paper TuA1-1.
 3. P.B. Hansen, L. Eskildsen, S.G. Grubb, A.J. Stentz, T.A. Strasser, J. Judkins, J.J. DeMarco, R. Pedrazzani, and D.J. DiGiovanni, "Capacity upgrades of transmission system by Raman amplifier", IEEE Photonics Technology Lett., Vol. 9, no. 2, pp. 262-264 (1997).
 4. R.H. Stolen, E.P. Ippen, and A.R. Tynes, "Raman oscillation in glass optical waveguide," Appl. Physics Lett., Vol. 20, no. 2, pp. 62-64 (1972).

CTuJ3 (Invited) 10:45 am

Recent advances in Raman amplification and applications

Howard Kidorf, *Lucent Tech., USA.*

Summary not available.

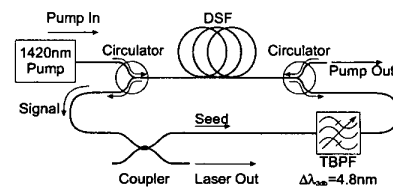
CTuJ4 11:15 am

Wavelength Tunable CW Raman Fiber Ring Laser Operating at 1486-1551 nm

P.C. Reeves-Hall and J.R. Taylor, *Femtosecond Optics Group, Department of Physics, Imperial College, London SW7 2BW; Email: pc.reeveshall@ic.ac.uk*

Erbium doped fiber lasers and amplifiers have provided a wealth of high power sources in the 1530 to 1580 nm spectral region. Other dopants such as Ytterbium and Thulium offer gain in other limited spectral regions but the non-linear effect of stimulated Raman scattering (SRS) provides for gain at any wavelength with the provision of a suitable pump source.^{1,2} Here we detail the optimization of a tunable fiber Raman ring laser with CW output between 1486 and 1551 nm, and use it to provide Raman gain over a tunable wavelength range of 1589 to 1650 nm.

The experimental configuration of our tunable wavelength, CW, Raman ring laser is shown in fig. 1. A cascaded Raman fiber laser with an output power of 1.58 W (post coupler) at 1420 nm was used as the pump source. Optical circulators, with a loss of <1 dB between 1450 and 1550 nm were used to mix and extract signal and pump wavelengths in a counter-propagating Raman amplifier configuration. This gave the advantage of removing pump radiation from the tunable laser output. Dispersion shifted fiber (DSF) was used as the Raman active medium



CTuJ4 Fig. 1. Experimental configuration of wavelength tunable CW Raman fiber ring laser.

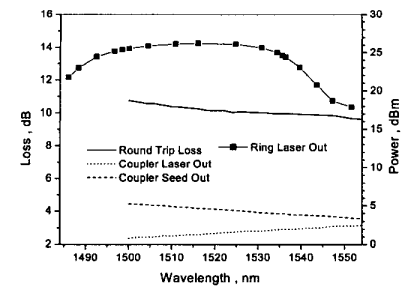
with the optimum length for high power output of the tunable laser determined experimentally. A broadband optical coupler was used to extract the tunable laser power and seed the ring laser, again, the coupling ratio was determined experimentally for optimum power output and wavelength tunability. A 4.8 nm tunable band pass filter (TBPF) was chosen for low loss (<0.8 dB) and extended wavelength tunability of 1456 to 1551 nm. The use of a broad bandpass filter reduces the detrimental effect of SBS in the gain fiber.

After optimization, the CW ring laser was used as a wavelength tunable pump source for a counter-propagating pump and signal Raman fiber amplifier with 20 km of standard telecommunications fiber (STF).

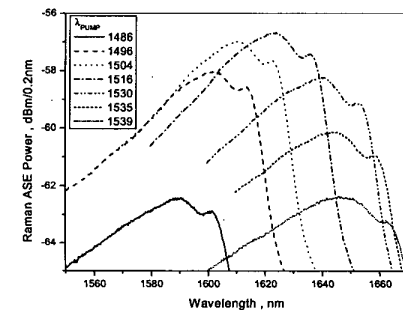
The optimum length of the DSF was experimentally determined to be of the order of 9 km. Optimum output was achieved using an optical coupler (attenuation <0.8 dB) with a 60:40 power ratio of laser output: seed. The transmission loss with wavelength of the optical coupler and round trip of the unpumped ring laser (without tunable filter) are shown in Fig. 2. The power output of the optimized ring laser with wavelength is also shown in Fig. 2.

The 3 dB line width of the ring laser output was around 1.5 nm for all tunable wavelengths. Peak output power was 420 mW at 1516 nm. The counter propagating pump and signal ASE spectra of a 20 km STF Raman fiber amplifier pumped using the CW wavelength tunable ring laser are shown in fig. 3.

The wavelength tunable Raman ring laser demonstrated here has a tuning range of 1486



CTuJ4 Fig. 2. Ring laser output power with wavelength, coupler and round trip losses with wavelength.



CTuJ4 Fig. 3. ASE power spectra of 20 km STF Raman fiber amplifier pumped with the CW wavelength tunable laser.

